Nonconforming Mixed Finite Element Approximations to Time-Harmonic Eddy Current Problems

P. Houston[1], I. Perugia[2] and D. Schötzau[3]

Abstract— **We present nonconforming mixed finite element methods for the discretization of time-harmonic eddy current problems. These methods are based on a discontinuous Galerkin approach, where the unknowns are approximated by completely discontinuous piecewise polynomials. In particular, we consider a stabilized mixed formulation involving equal-order elements, and a non-stabilized variant employing mixed-order elements.**

I. Introduction

In recent years, there has been considerable interest in nonconforming finite element methods that are based on discontinuous piecewise polynomial approximation spaces. Such approaches are referred to as discontinuous Galerkin (DG) methods (for a recent overview, see [1]). The main advantages of these methods lie in their conservation properties, their ability to treat a wide range of problems within the same unified framework, and their great flexibility in the mesh-design. Indeed, DG methods can naturally handle non-matching grids and non-uniform, even anisotropic, polynomial approximation degrees. Moreover, orthogonal bases can be constructed which lead to diagonal mass matrices; this is particularly advantageous in unsteady problems. Finally, in combination with block-type preconditioners, DG methods can easily be parallelized.

This paper deals with DG discretizations of mixed field- and potential-based formulations of eddy current problems in the time-harmonic regime. For the electric field formulation, the divergence-free constraint within non-conductive regions is imposed by means of a Lagrange multiplier. This allows for the correct capturing of edge and corner singularities in polyhedral domains; in contrast, additional Sobolev regularity must be assumed in the DG formulations of [2] and [3], when regularization techniques are employed. In particular, we present a mixed method involving equal-order discontinuous elements, which includes a normal jump stabilization term, and a non-stabilized variant, employing mixed-order discontinuous elements. The first formulation, introduced in [4], delivers optimal convergence rates for the vector-valued unknowns in a suitable energy norm. The second formulation, which can be viewed as a DG version of the mixed method of [5], is new; this latter scheme is designed to yield optimal convergence rates in both the L^2–norm, as well as in a suitable energy norm.

II. Model Problem

Given $\Omega \subset \mathbb{R}^3$, a simply connected bounded Lipschitz polyhedral domain with connected boundary $\partial\Omega$, we consider the problem: find the vector field $\boldsymbol{u}$ and the scalar field p such that

$$\begin{aligned} \nabla \times (\mu^{-1}\nabla \times \boldsymbol{u}) + \eta_1 \boldsymbol{u} + \eta_2 \nabla p = \boldsymbol{f} \quad & \text{in } \Omega, \\ \nabla \cdot (\eta_3\, \boldsymbol{u} + \eta_4 \nabla p) = 0 \quad & \text{in } \Omega, \end{aligned} \tag{1}$$

with suitable boundary conditions. Here, $\boldsymbol{f}$ is a given source field, and the coefficients μ and η_i, $i = 1, \ldots, 4$, are real functions (in all the cases below, μ is the magnetic permeability).

For $\eta_i = j\omega\sigma$, $i = 1, \ldots, 4$, where ω is a given frequency and σ the electric conductivity, problem (1) represents the $\boldsymbol{A}-V$ formulation of the time-harmonic eddy current problem [6] ($\boldsymbol{u} \equiv \boldsymbol{A}$, the magnetic vector potential, and $p \equiv V$, the electric scalar potential). For $\eta_1 = j\omega\sigma$, $\eta_4 = 0$ and $\eta_2 = -\eta_3 = -\varepsilon\chi_{\Omega_0}$, where ε is the electric permittivity and χ_{Ω_0} the characteristic function of the non-conducting subregion $\Omega_0 \subseteq \Omega$, problem (1) is a mixed electric field formulation of the time-harmonic eddy current problem ($\boldsymbol{u} \equiv \boldsymbol{E}$ and p is the Lagrange multiplier related to the divergence-free constraint in Ω_0). For $\eta_1 = \eta_4 = 0$ and $\eta_2 = -\eta_3 = -1$, (1) is a mixed magnetic vector potential formulation of the magnetostatic problem with Coulomb's gauge.

III. DG Formulations

We present two DG methods for the discretization of problem (1). For simplicity, we set $\eta_1 = \eta_4 = 0$, $\eta_2 = -\eta_3 = -1$, $\mu = 1$ and impose $\boldsymbol{n} \times \boldsymbol{u} = \boldsymbol{0}$ and $p = 0$ on $\partial\Omega$. The key difficulties in the numerical treatment of more general problems of type (1) are already present in this particular case.

A. Meshes, finite element spaces and trace operators

We consider conforming and shape regular meshes $\mathcal{T}_h$ that partition Ω into tetrahedra $\{K\}$. Let h_K be the diameter of $K \in \mathcal{T}_h$ and set $h = \max_K h_K$. We denote by $\mathcal{F}_h^{\mathcal{I}}$ and $\mathcal{F}_h^{\mathcal{B}}$ the union of all interior and boundary faces, respectively, and set $\mathcal{F}_h = \mathcal{F}_h^{\mathcal{I}} \cup \mathcal{F}_h^{\mathcal{B}}$. We define the *local mesh size* function $\mathtt{h}$ on $\mathcal{F}_h$ by setting $\mathtt{h}(\boldsymbol{x}) = \min\{h_{K^+}, h_{K^-}\}$, if $\boldsymbol{x}$ is in the interior of $\partial K^+ \cap \partial K^-$, and $\mathtt{h}(\boldsymbol{x}) = h_K$, if $\boldsymbol{x}$ is in the interior of $\partial K \cap \partial\Omega$.

The generic discontinuous finite element space is

$$P^\ell(\mathcal{T}_h) := \{u \in L^2(\Omega) : u|_K \in \mathbb{P}^\ell(K)\ \ \forall K \in \mathcal{T}_h\},$$

where $\mathbb{P}^\ell(K)$ is the space of polynomials of degree $\leq \ell$ on K.

For $f \subset \mathcal{F}_h^{\mathcal{I}}$ shared by two elements K^+ and K^- with outward unit normals $\boldsymbol{n}^\pm$, respectively, we define, with obvious notation, the *jumps* across f by $[\![\boldsymbol{v}]\!]_T = \boldsymbol{n}^+ \times \boldsymbol{v}^+ + \boldsymbol{n}^- \times \boldsymbol{v}^-$, $[\![\boldsymbol{v}]\!]_N = \boldsymbol{v}^+ \cdot \boldsymbol{n}^+ + \boldsymbol{v}^- \cdot \boldsymbol{n}^-$, $[\![q]\!]_N = q^+\boldsymbol{n}^+ + q^-\boldsymbol{n}^-$, and the *averages* by $\{\!\{\boldsymbol{v}\}\!\} = (\boldsymbol{v}^+ + \boldsymbol{v}^-)/2$ and $\{\!\{q\}\!\} = (q^+ + q^-)/2$. On $f \subset \mathcal{F}_h^{\mathcal{B}}$, we set $[\![\boldsymbol{v}]\!]_T = \boldsymbol{n} \times \boldsymbol{v}$, $[\![q]\!]_N = q\,\boldsymbol{n}$ and $\{\!\{\boldsymbol{v}\}\!\} = \boldsymbol{v}$.

B. Discontinuous Galerkin discretizations

For the finite element spaces $\boldsymbol{V}_h = P^\ell(\mathcal{T}_h)^3$ and $Q_h = P^m(\mathcal{T}_h)$ with $\ell, m \geq 1$, we introduce the following DG methods

[1]Department of Maths. & Computer Science, University of Leicester, Leicester LE1 7RH, UK. Email: Paul.Houston@mcs.le.ac.uk
(Funded by the EPSRC: Grant GR/R76615)
[2]Dipartimento di Matematica, Università di Pavia, Via Ferrata 1, 27100 Pavia, Italy. Email: perugia@dimat.unipv.it

[3]Department of Mathematics, University of Basel, Rheinsprung 21, 4051 Basel, Switzerland. Email: schotzau@math.unibas.ch

for problem (1): find $(\boldsymbol{u}_h, p_h) \in \boldsymbol{V}_h \times Q_h$ such that

$$a_h(\boldsymbol{u}_h, \boldsymbol{v}) + b_h(\boldsymbol{v}, p_h) = f_h(\boldsymbol{v}) \qquad \forall\, \boldsymbol{v} \in \boldsymbol{V}_h, \tag{2}$$

$$b_h(\boldsymbol{u}_h, q) - c_h(p_h, q) = 0 \qquad \forall\, q \in Q_h. \tag{3}$$

Here, a_h, b_h, c_h and f_h are defined, respectively, by

$$\begin{aligned} a_h(\boldsymbol{u}, \boldsymbol{v}) &= \int_\Omega \nabla_h \times \boldsymbol{u} \cdot \nabla_h \times \boldsymbol{v} \, d\boldsymbol{x} \\ &\quad - \int_{\mathcal{F}_h} \Big([\![\boldsymbol{u}]\!]_T \cdot \{\!\{\nabla_h \times \boldsymbol{v}\}\!\} + [\![\boldsymbol{v}]\!]_T \cdot \{\!\{\nabla_h \times \boldsymbol{u}\}\!\} \Big) \, ds \\ &\quad + \int_{\mathcal{F}_h} \mathtt{a} \, [\![\boldsymbol{u}]\!]_T \cdot [\![\boldsymbol{v}]\!]_T \, ds + \int_{\mathcal{F}_h^{\mathcal{I}}} \mathtt{b} \, [\![\boldsymbol{u}]\!]_N [\![\boldsymbol{v}]\!]_N \, ds, \\ b_h(\boldsymbol{v}, p) &= - \int_\Omega \boldsymbol{v} \cdot \nabla_h p \, d\boldsymbol{x} + \int_{\mathcal{F}_h} \{\!\{\boldsymbol{v}\}\!\} \cdot [\![p]\!]_N \, ds, \\ c_h(p, q) &= \int_{\mathcal{F}_h} \mathtt{c} \, [\![p]\!]_N \cdot [\![q]\!]_N \, ds, \qquad f_h(\boldsymbol{v}) = \int_\Omega \boldsymbol{f} \cdot \boldsymbol{v} \, d\boldsymbol{x}, \end{aligned}$$

with ∇_h denoting the elementwise "nabla" operator. The parameters $\mathtt{a}$ and $\mathtt{c}$ are strictly positive and proportional to $1/\mathtt{h}$; $\mathtt{b}$ is a non-negative parameter used to penalize normal jumps of $\boldsymbol{u}$. In particular, we consider the following two methods:

- **Method I (stabilized)**: we take $\mathtt{b} > 0$ and proportional to $\mathtt{h}$, and $m = \ell$ (equal-order polynomial spaces).
- **Method II (non-stabilized):** we take $\mathtt{b} = 0$, and $m = \ell + 1$ (mixed-order polynomial spaces), to ensure stability.

Remark 1: In order to deal with inhomogeneous Dirichlet boundary conditions $\boldsymbol{n} \times \boldsymbol{u} = \boldsymbol{g}$ on $\partial\Omega$, with $\boldsymbol{g}$ in $L^2(\partial\Omega)^3$, it is enough to modify the functional f_h as follows:

$$f_h(\boldsymbol{v}) = \int_\Omega \boldsymbol{f} \cdot \boldsymbol{v} \, d\boldsymbol{x} - \int_{\mathcal{F}_h^{\mathcal{B}}} \boldsymbol{g} \cdot \nabla_h \times \boldsymbol{v} \, ds - \int_{\mathcal{F}_h^{\mathcal{B}}} \mathtt{a} \boldsymbol{g} \cdot (\boldsymbol{n} \times \boldsymbol{v}) \, ds.$$

IV. Theoretical Results

Both Method I and Method II are well-posed and optimally convergent in an energy-like norm; this was shown in [4] for Method I, following the outline reported below. For Method II, we present here the main steps of the analysis; a complete proof of this result will be given in the forthcoming paper [7].

We set $\boldsymbol{V} = H_0(\mathrm{curl}; \Omega) \cap H(\mathrm{div}; \Omega)$, $Q = H_0^1(\Omega)$ and define $\boldsymbol{V}(h) = \boldsymbol{V} + \boldsymbol{V}_h$, $Q(h) = Q + Q_h$. We recall that $\boldsymbol{V}_h = P^\ell(\mathcal{T}_h)^3$ for both methods, whereas $Q_h = P^\ell(\mathcal{T}_h)$ for Method I and $Q_h = P^{\ell+1}(\mathcal{T}_h)$ for Method II.

We introduce the DG-seminorm and norms

$$\begin{aligned} |\boldsymbol{v}|^2_{\boldsymbol{V}(h)} &= \|\nabla_h \times \boldsymbol{v}\|^2_{0,\Omega} + \|\mathtt{h}^{-\frac{1}{2}} [\![\boldsymbol{v}]\!]_T\|^2_{0,\mathcal{F}_h} + \|\mathtt{b}^{\frac{1}{2}} [\![\boldsymbol{v}]\!]_N\|^2_{0,\mathcal{F}_h^{\mathcal{I}}}, \\ \|\boldsymbol{v}\|^2_{\boldsymbol{V}(h)} &= \|\boldsymbol{v}\|^2_{0,\Omega} + |\boldsymbol{v}|^2_{\boldsymbol{V}(h)}, \\ \|q\|^2_{Q(h)} &= \|\nabla_h q\|^2_{0,\Omega} + \|\mathtt{h}^{-\frac{1}{2}} [\![q]\!]_N\|^2_{0,\mathcal{F}_h}. \end{aligned}$$

Notice that the DG–seminorm and norm contain the normal jumps of functions in $\boldsymbol{V}(h)$ for Method I only.

Finally, we denote by $H^s(\Omega)$ the standard Sobolev space of regularity exponent $s > 0$, endowed with the usual norm $\|v\|_{s,\Omega}$.

The following theorem states error estimates for both Method I and Method II that are optimal with respect to the mesh size h, for each fixed ℓ.

Theorem 1: Assume that the analytical solution $(\boldsymbol{u}, p)$ to (1) satisfies $\boldsymbol{u} \in H^s(\Omega)^3$, $\nabla \times \boldsymbol{u} \in H^s(\Omega)^3$, and $p \in H^{s+1}(\Omega)$, for a regularity exponent $s > \frac{1}{2}$. Let $(\boldsymbol{u}_h, p_h)$ be the mixed DG approximation obtained by (2)–(3) either by Method I ($\mathtt{b} > 0$ and proportional to $\mathtt{h}$, and $m = \ell$) or by Method II ($\mathtt{b} = 0$ and $m = \ell + 1$) on conforming meshes. Then we have the a priori error bound

$$\begin{aligned} &\|\boldsymbol{u} - \boldsymbol{u}_h\|_{\boldsymbol{V}(h)} + \|p - p_h\|_{Q(h)} \\ &\qquad \le C\, h^{\min\{s,\ell\}} \Big[\|\boldsymbol{u}\|_{s,\Omega} + \|\nabla \times \boldsymbol{u}\|_{s,\Omega} + \|p\|_{s+1,\Omega} \Big], \end{aligned}$$

with a constant $C > 0$ independent of h.

Notice that the smoothness assumptions for $\boldsymbol{u}$ in Theorem 1 are minimal; see [8]. The assumption $p \in H^{s+1}(\Omega)$ is trivially satisfied in the physically most relevant case of divergence-free source terms $\boldsymbol{j}$, where $p \equiv 0$.

For Method I, the same convergence result as in Theorem 1 can be proven on meshes with hanging nodes, provided that the solution satisfies a slightly stronger regularity assumption [4].

Additionally, we note that the above Theorem also holds in the case when affine quadrilateral meshes are employed. In this case Method I is constructed using $(Q^\ell)^3 - Q^\ell$ elements; on the other hand for Method II we employ the discontinuous version of the first family of Nédélec's elements, cf. [9].

We point out that Method II seems to deliver better convergence rates for $\boldsymbol{u}$ in the L^2–norm, as shown in numerical results reported in Section V below. A theoretical justification of this result will be addressed elsewhere.

A. Outline of the Proof of Theorem 1 for Method I

We report here the main steps of the proof of Theorem 1 for Method I, following [4].

Step 1: Auxiliary mixed formulation. We rewrite the discrete formulation (2)–(3) in a different (and nonconforming) form, by introducing the jumps of p_h as auxiliary unknowns and by employing lifting operators as in [10], [2]. In this way, the resulting bilinear forms have suitable continuity and coercivity properties, so that the method can be analyzed by using the classical theory of mixed finite methods. More precisely, we introduce the lifting operators $\mathcal{L}$ and $\mathcal{M}$ as follows: for $\boldsymbol{v} \in \boldsymbol{V}(h)$ and $q \in Q(h)$, we define $\mathcal{L}(\boldsymbol{v}) \in \boldsymbol{V}_h$ and $\mathcal{M}(q) \in \boldsymbol{V}_h$ by

$$\begin{aligned} \int_\Omega \mathcal{L}(\boldsymbol{v}) \cdot \boldsymbol{w} \, d\boldsymbol{x} &= \int_{\mathcal{F}_h} [\![\boldsymbol{v}]\!]_T \cdot \{\!\{\boldsymbol{w}\}\!\} \, ds \qquad \forall \boldsymbol{w} \in \boldsymbol{V}_h, \\ \int_\Omega \mathcal{M}(q) \cdot \boldsymbol{w} \, d\boldsymbol{x} &= \int_{\mathcal{F}_h} \{\!\{\boldsymbol{w}\}\!\} \cdot [\![q]\!]_N \, ds \qquad \forall \boldsymbol{w} \in \boldsymbol{V}_h, \end{aligned}$$

respectively. Now we define the forms

$$\begin{aligned} \widetilde{a}_h(\boldsymbol{u}, \boldsymbol{v}) &= \int_\Omega \nabla_h \times \boldsymbol{u} \cdot \nabla_h \times \boldsymbol{v} \, d\boldsymbol{x} \\ &\quad - \int_\Omega \Big(\mathcal{L}(\boldsymbol{u}) \cdot (\nabla_h \times \boldsymbol{v}) + \mathcal{L}(\boldsymbol{v}) \cdot (\nabla_h \times \boldsymbol{u}) \Big) \, d\boldsymbol{x} \\ &\quad + \int_{\mathcal{F}_h} \mathtt{a} \, [\![\boldsymbol{u}]\!]_T \cdot [\![\boldsymbol{v}]\!]_T \, ds + \int_{\mathcal{F}_h^{\mathcal{I}}} \mathtt{b} \, [\![\boldsymbol{u}]\!]_N [\![\boldsymbol{v}]\!]_N \, ds, \\ \widetilde{b}_h(\boldsymbol{v}, p) &= - \int_\Omega \boldsymbol{v} \cdot \big(\nabla_h p - \mathcal{M}(p) \big) \, d\boldsymbol{x}. \end{aligned}$$

Note that $a_h = \widetilde{a}_h$ in $\boldsymbol{V}_h \times \boldsymbol{V}_h$ and $b_h = \widetilde{b}_h$ in $\boldsymbol{V}_h \times Q_h$, although this is no longer true in $\boldsymbol{V}(h) \times \boldsymbol{V}(h)$ and in $\boldsymbol{V}(h) \times Q(h)$, respectively. Next, we define the discrete space

$$M_h = \{\lambda \in L^2(\mathcal{F}_h) : \lambda|_f \in \mathbb{P}^\ell(f)^3 \ \ \forall f \subset \mathcal{F}_h\},$$

with $\mathbb{P}^\ell(f)$ denoting the polynomials of degree $\leq \ell$ on f, endowed with the norm $\|\eta\|_{M_h} = \|\mathtt{h}^{-\frac{1}{2}}\eta\|_{0,\mathcal{F}_h}$. We consider the following auxiliary mixed formulation: find $(\boldsymbol{u}_h, \lambda_h, p_h) \in \boldsymbol{V}_h \times M_h \times Q_h$ such that

$$\begin{aligned} &A_h(\boldsymbol{u}_h, \lambda_h; \boldsymbol{v}, \eta) + B_h(\boldsymbol{v}, \eta; p_h) = f_h(\boldsymbol{v}) \quad && \forall (\boldsymbol{v}, \eta) \in \boldsymbol{V}_h \times M_h, \\ &B_h(\boldsymbol{u}_h, \lambda_h; q) = 0 && \forall q \in Q_h, \end{aligned}$$

with forms A_h and B_h given by

$$A_h(\boldsymbol{u}, \lambda; \boldsymbol{v}, \eta) = \widetilde{a}_h(\boldsymbol{u}, \boldsymbol{v}) + \int_{\mathcal{F}_h} \mathtt{c}\lambda\eta \, ds,$$

$$B_h(\boldsymbol{v}, \eta; p) = \widetilde{b}_h(\boldsymbol{v}, p) - \int_{\mathcal{F}_h} \mathtt{c}[\![p]\!]_N \eta \, ds.$$

This auxiliary problem admits a unique solution $(\boldsymbol{u}_h, \lambda_h, p_h)$, with $(\boldsymbol{u}_h, p_h)$ the solution to (2)–(3), and $\lambda_h = [\![p_h]\!]_N$.

Step 2: Continuity properties. We introduce the space $\boldsymbol{W}(h) = \boldsymbol{V}(h) \times M_h$ and the product norm

$$\|(\boldsymbol{v}, \eta)\|^2_{\boldsymbol{W}(h)} = \|\boldsymbol{v}\|^2_{\boldsymbol{V}(h)} + \|\eta\|^2_{M_h}.$$

By using the stability estimates for the lifting operators

$$\|\mathcal{L}(\boldsymbol{v})\|_{0,\Omega} \leq C_{\text{lift}} \|\mathtt{h}^{-\frac{1}{2}} [\![\boldsymbol{v}]\!]_T\|_{0,\mathcal{F}_h},$$

$$\|\mathcal{M}(q)\|_{0,\Omega} \leq C_{\text{lift}} \|\mathtt{h}^{-\frac{1}{2}} [\![q]\!]_N\|_{0,\mathcal{F}_h},$$

with $C_{\text{lift}} > 0$ independent of h, the following continuity properties can be proved: there exist constants $a_1 > 0$ and $a_2 > 0$ independent of h such that, for any $(\boldsymbol{u}, \lambda), (\boldsymbol{v}, \eta) \in \boldsymbol{W}(h)$ and $q \in Q(h)$,

$$|A_h(\boldsymbol{u}, \lambda; \boldsymbol{v}, \eta)| \leq a_1 \, \|(\boldsymbol{u}, \lambda)\|_{\boldsymbol{W}(h)} \|(\boldsymbol{v}, \eta)\|_{\boldsymbol{W}(h)},$$

$$|B_h(\boldsymbol{v}, \eta; q)| \leq a_2 \, \|(\boldsymbol{v}, \eta)\|_{\boldsymbol{W}(h)} \|q\|_{Q(h)}.$$

Step 3: Ellipticity on the kernel. Define the discrete kernel $\mathrm{Ker}(B_h) = \{(\boldsymbol{u}, \lambda) \in \boldsymbol{W}_h : B_h(\boldsymbol{u}, \lambda; p) = 0 \ \forall p \in Q_h\}$. By using a duality argument, the following ellipticity property can be proved: there exists a constant $b > 0$ independent of h such that, for any $(\boldsymbol{u}, \lambda) \in \mathrm{Ker}(B_h)$,

$$A_h(\boldsymbol{u}, \lambda; \boldsymbol{u}, \lambda) \geq b \, \|(\boldsymbol{u}, \lambda)\|^2_{\boldsymbol{W}(h)},$$

provided that the coefficient α in the definition of the interior penalty parameter $\mathtt{a} := \alpha/\mathtt{h}$ is large enough (this restriction is typical of symmetric interior penalty methods).

Step 4: Inf-sup condition. We have

$$\inf_{0 \neq q \in Q_h} \sup_{\boldsymbol{0} \neq (\boldsymbol{v}, \nu) \in \boldsymbol{W}_h} \frac{B_h(\boldsymbol{v}, \nu; q)}{\|q\|_{Q(h)} \|(\boldsymbol{v}, \nu)\|_{\boldsymbol{W}(h)}} \geq \kappa > 0$$

for a constant κ independent of h. The proof of this result which was carried out in [4] is inspired by recent ideas from [11] used in the analysis of stabilized mixed methods, and makes use of the following norm equivalence: let Q_h^c be the subspace $Q_h \cap H_0^1(\Omega)$ of Q_h, and let $Q_h^\perp$ be its $Q(h)$–orthogonal complement in Q_h; define $\|q\|_{Q_h^\perp} := \|\mathtt{h}^{-\frac{1}{2}} [\![q]\!]_N\|_{0,\mathcal{F}_h}$ (we observe that $\|q\|_{Q_h^\perp}$ is actually a norm on $Q_h^\perp$); then there exists a constant $C \geq 1$ independent of h such that $C^{-1} \|q\|_{Q(h)} \leq \|q\|_{Q_h^\perp} \leq C \|q\|_{Q(h)}$, for any $q \in Q_h^\perp$.

Step 5: Abstract error estimates. For the exact solution $(\boldsymbol{u}, p)$ to (1), we define the residuals

$$\begin{aligned} R_h^1(\boldsymbol{u}, p; \boldsymbol{v}, \nu) &= A_h(\boldsymbol{u}, 0; \boldsymbol{v}, \nu) + B_h(\boldsymbol{v}, \nu; p) - f_h(\boldsymbol{v}), \\ R_h^2(\boldsymbol{u}; q) &= B_h(\boldsymbol{u}, 0; q) \end{aligned}$$

for all $(\boldsymbol{v}, \nu) \in \boldsymbol{W}_h$ and $q \in Q_h$, and set

$$\mathcal{R}_h^1(\boldsymbol{u}, p) = \sup_{\boldsymbol{0} \neq (\boldsymbol{v}, \nu) \in \boldsymbol{W}_h} \frac{|R_h^1(\boldsymbol{u}, p; \boldsymbol{v}, \nu)|}{\|(\boldsymbol{v}, \nu)\|_{\boldsymbol{W}(h)}},$$

$$\mathcal{R}_h^2(\boldsymbol{u}) = \sup_{0 \neq q \in Q_h} \frac{|R_h^2(\boldsymbol{u}; q)|}{\|q\|_{Q(h)}}.$$

The following abstract error estimates for our DG method are obtained by straightforwardly extending the standard conforming mixed finite element theory [12] to the setting considered here, and taking into account the residual terms arising from the nonconformity: there exist constants $C > 0$ depending on the constants a_1, a_2, b and the inf-sup constant κ, but independent of the mesh size h, such that

$$\|(\boldsymbol{u} - \boldsymbol{u}_h, \lambda_h)\|_{\boldsymbol{W}(h)} \leq C \Big[\inf_{\boldsymbol{v} \in \boldsymbol{V}_h} \|\boldsymbol{u} - \boldsymbol{v}\|_{\boldsymbol{V}(h)} + \inf_{q \in Q_h} \|p - q\|_{Q(h)} + \mathcal{R}_h^1(\boldsymbol{u}, p) + \mathcal{R}_h^2(\boldsymbol{u}) \Big],$$

and

$$\|p - p_h\|_{Q(h)} \leq C \Big[\inf_{q \in Q_h} \|p - q\|_{Q(h)} + \|(\boldsymbol{u} - \boldsymbol{u}_h, \lambda_h)\|_{\boldsymbol{W}(h)} + \mathcal{R}_h^1(\boldsymbol{u}, p) \Big].$$

Step 6: Proof of Theorem 1. First, one can show that the residuals are optimally convergent:

$$\mathcal{R}_h^1(\boldsymbol{u}, p) + \mathcal{R}_h^2(\boldsymbol{u}) \leq C h^{\min\{s, \ell+1\}} \big[\|\boldsymbol{u}\|_{s,\Omega} + \|\nabla \times \boldsymbol{u}\|_{s,\Omega}\big],$$

with a constant $C > 0$ independent of h. Further, we can choose $\boldsymbol{v} = \boldsymbol{\Pi}_{\text{curl}} \boldsymbol{u} \in H_0(\text{curl}; \Omega)$ and $q = \Pi_{H^1} p \in H_0^1(\Omega)$ in the abstract error estimates of Step 5, where $\boldsymbol{\Pi}_{\text{curl}}$ is the standard conforming Nédéléc interpolant of the second type [13], and Π_{H^1} is a standard H^1–projector. Therefore, $[\![\boldsymbol{v}]\!]_T = \boldsymbol{0}$ on $\mathcal{F}_h$ and $[\![q]\!]_N = 0$ on $\mathcal{F}_h$. Since it can also be shown that

$$\|\mathtt{h}^{\frac{1}{2}} [\![\boldsymbol{u} - \boldsymbol{v}]\!]_N\|_{0,\mathcal{F}_h^{\mathcal{I}}} \leq C \, h^{\min\{s, \ell\}} \big[\|\boldsymbol{u}\|_{s,\Omega} + \|\nabla \times \boldsymbol{u}\|_{s,\Omega}\big],$$

we obtain

$$\|\boldsymbol{u} - \boldsymbol{v}\|_{\boldsymbol{V}(h)} \leq C \, h^{\min\{s, \ell\}} \big[\|\boldsymbol{u}\|_{s,\Omega} + \|\nabla \times \boldsymbol{u}\|_{s,\Omega}\big]$$

(see [14]), and

$$\|p - q\|_{Q(h)} \leq C \, h^{\min\{s, \ell\}} \|p\|_{s+1,\Omega}.$$

Inserting these estimates, together with the estimates of the residuals, in the previous abstract estimates gives the result.

B. Outline of the Proof of Theorem 1 for Method II

The analysis of Method II is based on an orthogonal decomposition of the discontinuous spaces $\boldsymbol{V}_h$ and Q_h and, as in [11], uses stability results for the underlying conforming spaces.

Step 1: Auxiliary formulation. We consider the following auxiliary formulation:

$$\begin{aligned} \widetilde{a}_h(\boldsymbol{u}_h, \boldsymbol{v}) + \widetilde{b}_h(\boldsymbol{v}, p_h) &= f_h(\boldsymbol{v}) && \forall\, \boldsymbol{v} \in \boldsymbol{V}_h, \\ \widetilde{b}_h(\boldsymbol{u}_h, q) - c_h(p_h, q) &= 0 && \forall\, q \in Q_h, \end{aligned}$$

where $\widetilde{a}_h$ and $\widetilde{b}_h$ are defined as in Step 1 for Method I (here, with $\mathtt{b} = 0$).

Step 2: Decomposition of discontinuous spaces. We decompose the spaces $\boldsymbol{V}_h$ and Q_h into

$$\boldsymbol{V}_h = \boldsymbol{V}_h^c \oplus \boldsymbol{V}_h^\perp, \qquad Q_h = Q_h^c \oplus Q_h^\perp, \tag{4}$$

where $\boldsymbol{V}_h^c = \boldsymbol{V}_h \cap H_0(\mathrm{curl};\Omega)$ is the Nédélec space of second type, with zero tangential trace on $\partial\Omega$, and $\boldsymbol{V}_h^\perp$ is its $\boldsymbol{V}(h)$–orthogonal complement in $\boldsymbol{V}_h$; similarly, $Q_h^c = Q_h \cap H_0^1(\Omega)$ is the space of continuous polynomials of degree or $\ell+1$, with zero trace on $\partial\Omega$, and $Q_h^\perp$ is its $Q(h)$–orthogonal complement in Q_h. We observe that the expressions $\|\boldsymbol{v}\|_{\boldsymbol{V}_h^\perp} := \|\mathtt{h}^{-\frac{1}{2}}[\![\boldsymbol{v}]\!]_T\|_{0,\mathcal{F}_h}$ and $\|q\|_{Q_h^\perp} := \|\mathtt{h}^{-\frac{1}{2}}[\![p]\!]_N\|_{0,\mathcal{F}_h}$ define norms in $\boldsymbol{V}_h^\perp$ and $Q_h^\perp$, respectively. The following norm-equivalence result will be at the basis of our analysis: there exist constants $C_1, C_2 \geq 1$ independent of h such that

$$\begin{aligned} C_1^{-1}\|\boldsymbol{v}\|_{\boldsymbol{V}(h)} &\leq \|\boldsymbol{v}\|_{\boldsymbol{V}_h^\perp} \leq C_1\|\boldsymbol{v}\|_{\boldsymbol{V}(h)}, \\ C_2^{-1}\|q\|_{Q(h)} &\leq \|q\|_{Q_h^\perp} \leq C_2\|q\|_{Q(h)}, \end{aligned}$$

for all $\boldsymbol{v} \in \boldsymbol{V}_h^\perp$ and all $q \in Q_h^\perp$, respectively.

Step 3: Continuity and coercivity properties. Recall that the forms $\widetilde{a}_h : \boldsymbol{V}(h) \times \boldsymbol{V}(h) \to \mathbb{R}$ and $\widetilde{b}_h : \boldsymbol{V}(h) \times Q(h) \to \mathbb{R}$ are continuous with continuity constants independent of h; moreover, $\widetilde{a}_h(\boldsymbol{v}, \boldsymbol{v}) \geq C\,|\boldsymbol{v}|^2_{\boldsymbol{V}(h)}$ for all $\boldsymbol{v} \in \boldsymbol{V}_h$, with a constant $C > 0$ independent of h, provided that the coefficient α in the definition of the stabilization parameter $\mathtt{a} = \alpha/\mathtt{h}$ is sufficiently large. The proof of these properties relies upon the same arguments as in Steps 2 and 3 for Method I.

Step 4: Stability properties. We recall the following stability properties of the forms $\widetilde{a}_h$ and $\widetilde{b}_h$ on the underlying conforming spaces $\boldsymbol{V}_h^c$ and Q_h^c in decomposition (4):

- There is a constant $b > 0$ independent of h such that

$$\widetilde{a}_h(\boldsymbol{v}, \boldsymbol{v}) \geq b\,\|\boldsymbol{v}\|^2_{\boldsymbol{V}(h)} \qquad \forall \boldsymbol{v} \in \boldsymbol{V}_h^c \cap \boldsymbol{Z}_h,$$

where $\boldsymbol{Z}_h := \{\boldsymbol{v} \in \boldsymbol{V}_h : b_h(\boldsymbol{v}, q) = 0,\ \forall q \in Q_h^c\}$.

- The inf-sup condition

$$\inf_{0 \neq q \in Q_h^c} \sup_{\boldsymbol{0} \neq \boldsymbol{v} \in \boldsymbol{V}_h^c} \frac{\widetilde{b}_h(\boldsymbol{v}, q)}{\|\boldsymbol{v}\|_{\boldsymbol{V}(h)}\|q\|_{Q(h)}} \geq \kappa > 0$$

holds true, with a constant κ independent of h.
Since $\boldsymbol{V}_h^c \subset \boldsymbol{V}_h$, the inf-sup condition also holds true with the same inf-sup constant when $\boldsymbol{V}_h^c$ is replaced by $\boldsymbol{V}_h$.

Step 5: A bound for $\|\boldsymbol{u}_h^\perp\|_{\boldsymbol{V}(h)}$ and $\|q_h^\perp\|_{Q(h)}$. Consider the decompositions $\boldsymbol{u}_h = \boldsymbol{u}_h^c + \boldsymbol{u}_h^\perp$ and $q_h = q_h^c + q_h^\perp$ of the components $\boldsymbol{u}_h$ and p_h of the solution to (2)–(3), according to (4). Then, for any real $\delta > 0$, there exists a constant $C_\delta > 0$, independent of h, such that

$$\begin{aligned} \|\boldsymbol{u}_h^\perp\|^2_{\boldsymbol{V}(h)} + \|q_h^\perp\|^2_{Q(h)} &\leq \delta^{-1}\|\boldsymbol{u} - \boldsymbol{u}_h\|^2_{\boldsymbol{V}(h)} \\ &\quad + C_\delta\left[\|\boldsymbol{u} - \boldsymbol{v}\|^2_{\boldsymbol{V}(h)} + \|p - q\|^2_{Q(h)} + \mathcal{E}(\boldsymbol{u})^2\right] \end{aligned}$$

for all $\boldsymbol{v} \in \boldsymbol{V}_h^c$ and all $q \in Q_h^c$. Here

$$\begin{aligned} \mathcal{E}(\boldsymbol{u})^2 = \sum_{K \in \mathcal{T}_h} h_K \Big[&\|\nabla \times \boldsymbol{u} - \boldsymbol{\Pi}_{\boldsymbol{V}_h}(\nabla \times \boldsymbol{u})\|^2_{0,\partial K} \\ &+ \|\boldsymbol{u} - \boldsymbol{\Pi}_{\boldsymbol{V}_h}(\boldsymbol{u})\|^2_{0,\partial K}\Big], \end{aligned}$$

$\boldsymbol{\Pi}_{\boldsymbol{V}_h}$ being the L^2–projection onto $\boldsymbol{V}_h$. This estimate can be obtained first by proving it for $(\boldsymbol{v}, q) \in \boldsymbol{V}_h^c \cap \boldsymbol{Z}_h \times Q_h^c$ and then by extending it to general $(\boldsymbol{v}, q) \in \boldsymbol{V}_h^c \times Q_h^c$ by using the inf-sup condition of Step 4. The norm equivalence of Step 2 and the curl-conformity of $\boldsymbol{u}_h^c$ are used in the first part of the proof.

Step 6: Abstract error estimates. Owing to decomposition (4), we can write $\|\boldsymbol{u} - \boldsymbol{u}_h\|^2_{\boldsymbol{V}(h)} \leq C\|\boldsymbol{u} - \boldsymbol{u}_h^c\|^2_{\boldsymbol{V}(h)} + C\|\boldsymbol{u}_h^\perp\|^2_{\boldsymbol{V}(h)}$. The term $\|\boldsymbol{u} - \boldsymbol{u}_h^c\|_{\boldsymbol{V}(h)}$ can be estimated by

$$\begin{aligned} \|\boldsymbol{u} - \boldsymbol{u}_h^c\|^2_{\boldsymbol{V}(h)} \leq C\Big[&\|\boldsymbol{u} - \boldsymbol{v}\|^2_{\boldsymbol{V}(h)} + \|p - q\|^2_{Q(h)} \\ &+ \|\boldsymbol{u}_h^\perp\|^2_{\boldsymbol{V}(h)} + \|p_h^\perp\|^2_{Q(h)}\Big], \end{aligned}$$

for all $\boldsymbol{v} \in \boldsymbol{V}_h^c$ that satisfy $\widetilde{b}_h(\boldsymbol{v}, r) = -\widetilde{b}_h(\boldsymbol{u}_h^\perp, r)$ for all $r \in Q_h^c$, and all $q \in Q_h^c$, and therefore

$$\begin{aligned} \|\boldsymbol{u} - \boldsymbol{u}_h\|^2_{\boldsymbol{V}(h)} \leq C\Big[&\|\boldsymbol{u} - \boldsymbol{v}\|^2_{\boldsymbol{V}(h)} + \|p - q\|^2_{Q(h)} \\ &+ \|\boldsymbol{u}_h^\perp\|^2_{\boldsymbol{V}(h)} + \|p_h^\perp\|^2_{Q(h)}\Big] \end{aligned}$$

for all $\boldsymbol{v}$ as above and all $q \in Q_h^c$. The result is then extended to all $\boldsymbol{v} \in \boldsymbol{V}_h^c$, and the bounds in Step 5 allow us to conclude that

$$\|\boldsymbol{u} - \boldsymbol{u}_h\|^2_{\boldsymbol{V}(h)} \leq C\left[\|\boldsymbol{u} - \boldsymbol{v}\|^2_{\boldsymbol{V}(h)} + \|p - q\|^2_{Q(h)} + \mathcal{E}(\boldsymbol{u})^2\right]$$

for all $\boldsymbol{v} \in \boldsymbol{V}_h^c$ and all $q \in Q_h^c$, with $C > 0$ independent of h.

The proof of the error bound

$$\|p - p_h\|^2_{Q(h)} \leq C\left[\|\boldsymbol{u} - \boldsymbol{v}\|^2_{\boldsymbol{V}(h)} + \|p - q\|^2_{Q(h)} + \mathcal{E}(\boldsymbol{u})^2\right]$$

for all $\boldsymbol{v} \in \boldsymbol{V}_h^c$ and all $q \in Q_h^c$, with $C > 0$ independent of h, is a straightforward extension of the analogous one for conforming mixed methods.

Step 7: Proof of Theorem 1. We choose $\boldsymbol{v}$ and q in the abstract error estimates of Step 6 as conforming projections of $\boldsymbol{u}$ and p, respectively. Standard interpolation estimates, together with the approximation properties of the L^2–projection needed for estimating $\mathcal{E}(\boldsymbol{u})$, give the result.

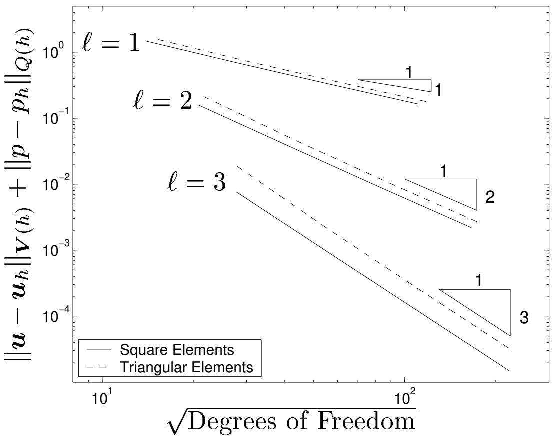

Fig. 1. *Example 1.* Method I: Convergence of $\|\boldsymbol{u} - \boldsymbol{u}_h\|_{\boldsymbol{V}(h)} + \|p - p_h\|_{Q(h)}$.

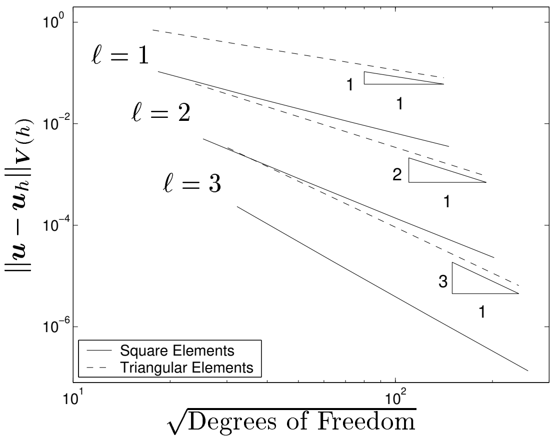

Fig. 2. *Example 1.* Method II: Convergence of $\|\boldsymbol{u} - \boldsymbol{u}_h\|_{\boldsymbol{V}(h)}$.

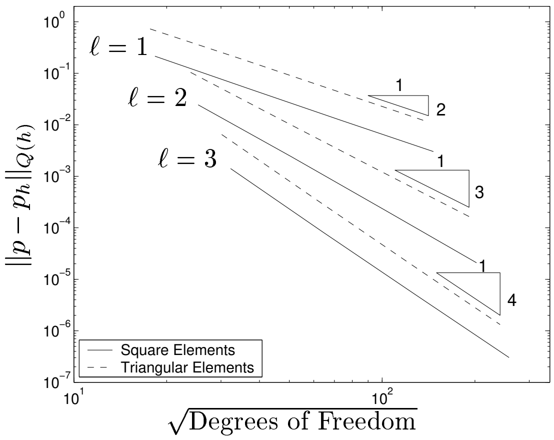

Fig. 3. *Example 1.* Method II: Convergence of $\|p - p_h\|_{Q(h)}$.

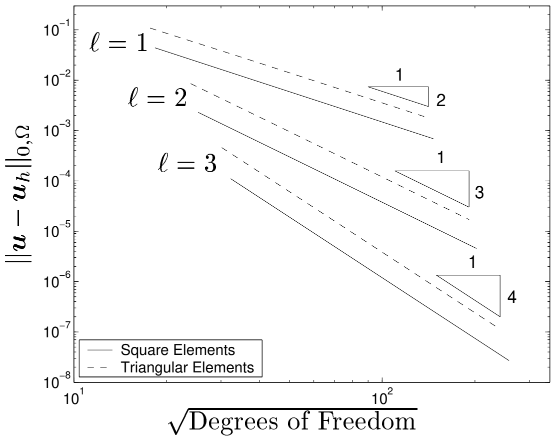

Fig. 4. *Example 1.* Method II: Convergence of $\|\boldsymbol{u} - \boldsymbol{u}_h\|_{0,\Omega}$.

V. Numerical Results

In this section we present a series of numerical experiments to highlight the practical performance of each of the nonconforming mixed methods introduced in this article for the numerical approximation of the model problem (1). In each case we select the parameters arising in (2)–(3). as follows: $\mathtt{a} = 10\ell^2/h$ and $\mathtt{c} = 1/h$ for both Methods I and II, while $\mathtt{b} = h$ for Method I and $\mathtt{b} = 0$ for Method II.

A. Example 1

In this first example, we let $\Omega = (-1,1)^2$ and select $\mathbf{f}$ so that the analytical solution to (1) is given by $\boldsymbol{u} = (-\exp(x)(y\cos(y) + \sin(y)), \exp(x)y\sin(y))$ and $p = \sin(\pi(x-1)/2)\sin(\pi(y-1)/2)$. Here, we investigate the asymptotic convergence of both methods on a sequence of successively finer uniform square and quasi-uniform unstructured triangular meshes for $\ell = 1, 2, 3$.

In Fig. 1 we first present a comparison of the sum of the DG–norms $\|\boldsymbol{u}-\boldsymbol{u}_h\|_{\boldsymbol{V}(h)}$ and $\|p-p_h\|_{Q(h)}$ with respect to the square root of the number of degrees of freedom in the finite element space $\boldsymbol{V}_h \times Q_h$ for the first (stabilized) method; for brevity, we have not shown these quantities individually, since for this equal-order method, each of these norms of the error converges to zero at the same rate. Indeed, here we observe convergence, for each fixed ℓ, at the optimal rate $\mathcal{O}(h^\ell)$ as the mesh is refined, thereby confirming Theorem 1. We remark that here we are only interested in demonstrating the general performance of the underlying method on meshes comprising of either square or triangular elements, but not in making a formal comparison of the accuracy of the scheme with respect to each element type. Indeed, although for each fixed ℓ we observe that the error on the uniform square meshes is smaller than the corresponding quantity measured on triangular meshes, the former meshes consist of uniform structured meshes, where we anticipate that local error cancellation will lead to a reduction in the size of the global error. On the other hand, the triangular meshes are completely unstructured, so we do not expect the same level of local error cancellation.

In Figs. 2 & 3 we plot the DG–norms $\|\cdot\|_{\boldsymbol{V}(h)}$ and $\|\cdot\|_{Q(h)}$ of the errors $\boldsymbol{u} - \boldsymbol{u}_h$ and $p - p_h$, respectively, as the mesh size tends to zero for Method II. As for Method I, we again observe that $\|\boldsymbol{u} - \boldsymbol{u}_h\|_{\boldsymbol{V}(h)}$ converges to zero, for each fixed ℓ, at the optimal rate $\mathcal{O}(h^\ell)$, as the mesh is refined, in accordance with Theorem 1. On the other hand, for this mixed-order method, $\|p - p_h\|_{Q(h)}$ converges at the rate $\mathcal{O}(h^{\ell+1})$, for each ℓ, as h tends to zero; this rate is indeed optimal, though this is not reflected by Theorem 1.

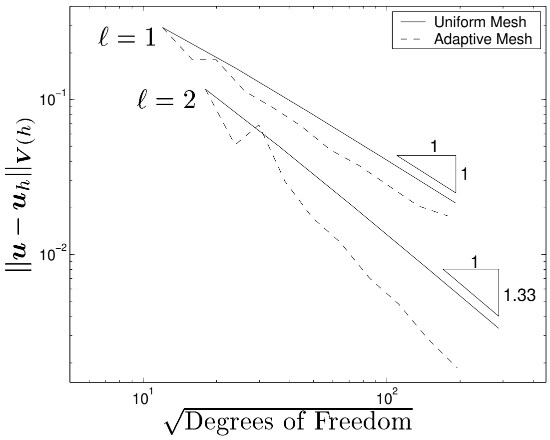

Fig. 5. *Example 2.* Method I: Convergence of $\|\boldsymbol{u} - \boldsymbol{u}_h\|_{\boldsymbol{V}(h)}$.

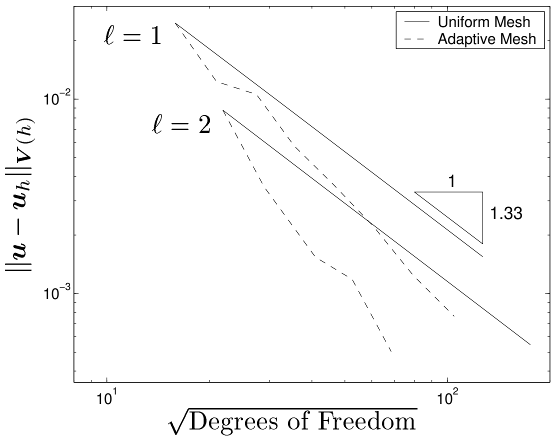

Fig. 6. *Example 2.* Method II: Convergence of $\|\boldsymbol{u} - \boldsymbol{u}_h\|_{\boldsymbol{V}(h)}$.

Finally, we highlight the optimality of Method II when the error in the computed vector field $\boldsymbol{u}_h$ is measure in terms of the $L^2(\Omega)$-norm. As noted in [4], $\|\boldsymbol{u}-\boldsymbol{u}_h\|_{0,\Omega}$ converges at the sub-optimal rate $\mathcal{O}(h^\ell)$, for each ℓ, as h tends to zero when Method I is employed. On the other hand, Fig. 4 demonstrates that the mixed-order method (Method II) yields an optimal convergence rate for the above quantity as the mesh is refined.

B. Example 2

We select $\Omega \subset \mathbb{R}^2$ to be the L–shaped domain with vertices $(1,0)$, $(1,1)$, $(-1,1)$, $(-1,-1)$, $(0,-1)$ and $(0,0)$. Furthermore, we set $\mathbf{f} = \mathbf{0}$ and impose $\boldsymbol{n} \times \boldsymbol{u} = \boldsymbol{g}$ and $p = 0$ on $\partial\Omega$, where $\boldsymbol{g}$ is chosen so that $\boldsymbol{u}(x,y) = \nabla(r^{4/3}\sin(4\vartheta/3))$, in terms of the polar coordinates (r,ϑ); thereby, $\mathbf{u} \in H^{4/3-\varepsilon}(\Omega)^2$, $\varepsilon > 0$. In this second example, we investigate the performance of both methods on uniform square and adaptively refined quadrilateral meshes where hanging nodes are introduced during the course of the refinement procedure. The adaptive meshes are constructed by employing the fixed fraction strategy (ref.: 25%, deref.: 0%) with a simple error indicator based on the gradient of the numerical approximation, cf. [4].

Fig. 5 presents a comparison of $\|\boldsymbol{u} - \boldsymbol{u}_h\|_{\boldsymbol{V}(h)}$ using the stabilized method (Method I) with the square root of the number of degrees of freedom in $\boldsymbol{V}_h \times Q_h$, for $\ell = 1, 2$. Here, we observe that $\|\boldsymbol{u} - \boldsymbol{u}_h\|_{\boldsymbol{V}(h)}$ converges to zero at the optimal rate $\min(s,\ell)$, $s = 4/3-\varepsilon$, $\varepsilon > 0$; cf. Section IV. Fig. 6 shows the corresponding comparison for the non-stabilized method (Method II); in this case, we clearly see that $\|\boldsymbol{u} - \boldsymbol{u}_h\|_{\boldsymbol{V}(h)}$ converges at the optimal rate s when both $\ell = 1$ and $\ell = 2$. We note that the adaptive meshes with hanging nodes are easily handled by the DG approach; indeed, from Figs. 5 & 6, we observe that the adaptively refined meshes lead to a general improvement in the error when compared to the uniform square meshes. Analogous results hold for the methods on uniform and adaptively refined triangular meshes; for brevity, these numerics are omitted.

VI. Conclusions

Based on the DG methodology, we have considered two nonconforming mixed finite element methods for the discretization of time-harmonic eddy current problems. Optimal order *a-priori* bounds in an energy-like norm have been presented and demonstrated numerically. We have highlighted the advantages of these methods by illustrating the performance of both schemes on adaptively refined meshes with hanging nodes. Future work will include extensions to *hp*–adaptive finite element methods.

References

[1] B. Cockburn, G.E. Karniadakis, and C.-W. Shu, eds. *Discontinuous Galerkin Methods. Theory, Computation and Applications*, vol. 11 of *Lect. Notes Comput. Sci. Eng.* Springer–Verlag, 2000.

[2] I. Perugia and D. Schötzau. The *hp*-local discontinuous Galerkin method for low-frequency time-harmonic Maxwell equations. *Math. Comp.* 72:1179–1214, 2003.

[3] P. Houston, I. Perugia, and D. Schötzau. *hp*-DGFEM for Maxwell's equations. In F. Brezzi, A. Buffa, S. Corsaro and A. Murli, editors, Numerical Mathematics and Advanced Applications ENUMATH 2001, pp. 785–794, Springer-Verlag, 2003.

[4] P. Houston, I. Perugia, and D. Schötzau. Mixed discontinuous Galerkin approximation of the Maxwell operator. Submitted.

[5] L. Demkowicz and L. Vardapetyan. Modeling of electromagnetic absorption/scattering problems using *hp*–adaptive finite elements. *Comput. Meth. Appl. Mech. Engrg.*, vol. 152, pp. 103-124, 1998.

[6] O. Biro. Edge element formulations of eddy current problems. *Comput. Methods Appl. Mech. Engrg.*, vol. 169, pp. 391-405, 1999.

[7] P. Houston, I. Perugia, and D. Schötzau. Mixed discontinuous Galerkin approximation of the Maxwell operator: non-stabilized formulations. In preparation.

[8] C. Amrouche, C. Bernardi, M. Dauge, and V. Girault. Vector potentials in three-dimensional non-smooth domains. *Math. Models Appl. Sci.*, 21:823–864, 1998.

[9] J.C. Nédélec. Mixed finite elements in $\mathbb{R}^3$. *Numer. Math.*, 55:315–341, 1980.

[10] D.N. Arnold, F. Brezzi, B. Cockburn, and L.D. Marini. Unified analysis of discontinuous Galerkin methods for elliptic problems. *SIAM J. Numer. Anal.*, 39:1749–1779, 2001.

[11] F. Brezzi and M. Fortin. A minimal stabilisation procedure for mixed finite element methods. *Numer. Math.*, 89:457–491, 2001.

[12] F. Brezzi and M. Fortin. Mixed and hybrid finite element methods. In *Springer Series in Computational Mathematics*, volume 15. Springer–Verlag, New York, 1991.

[13] J.C. Nédélec. A new family of mixed finite elements in $\mathbb{R}^3$. *Numer. Math.*, 50:57–81, 1986.

[14] A. Alonso and A. Valli. An optimal domain decomposition preconditioner for low-frequency time-harmonic Maxwell equations. *Math. Comp.*, 68:607–631, 1999.